

Exploring QSAR of peripheral benzodiazepine receptor binding affinity of 2-phenylpyrazolo[1,5-a]pyrimidin-3-yl-acetamides using topological and physicochemical descriptors

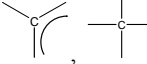
Manoj Kumar Dalai, J Thomas Leonard & Kunal Roy*

Drug Theoretics & Cheminformatics Lab, Division of Medicinal & Pharmaceutical Chemistry
Department of Pharmaceutical Technology, Jadavpur University, Kolkata 700 032, India

E-mail: kunalroy_in@yahoo.com

Received 3 January 2006; accepted (revised) 22 June 2006

The structural and physicochemical requirements of 2-phenylpyrazolo[1,5-a]pyrimidin-3-yl-acetamides for binding with peripheral benzodiazepine receptor has been explored in the present QSAR study. The calculated hydrophobicity, $\log P_{\text{calc}}$, shows a parabolic relation with the peripheral benzodiazepine receptor binding affinity, which suggests that the binding affinity increases with increase in the partition coefficient of the compounds until it reaches the critical value after which the affinity decreases. The range of the optimum values of $\log P_{\text{calc}}$ is between 5.423-5.819 as found from different equations. The width of the *para* substituents at R_3 position is conducive for the binding affinity. The E-state values of the fragments

like methyl,  and  are conducive for the binding affinity, while E-state value of the fragment -F is detrimental to the binding affinity. The average distance sum of the connectivity (Balaban J) among different groups is also conducive for the binding affinity. The presence of methyl groups at R_1 and R_2 positions and the presence of substituents at R_5 position are detrimental to the binding affinity, while presence of substituents at R_3 position and the presence of methyl group at R_6 position are conducive to the binding affinity.

Keywords: QSAR study, peripheral benzodiazepine, receptor, 2-phenylpyrazolo[1,5-a]pyrimidine

IPC Code: Int. Cl.⁸ C07D

Benzodiazepines are among the most widely prescribed drugs due to their pharmacological actions in relieving anxiety, and as anticonvulsants, muscle relaxants, or sedative hypnotics. These effects are mediated in the central nervous system through postsynaptic plasma membrane GABA_A receptors that are γ -amino butyric acid-gated chloride channels¹. Benzodiazepines bind with two main classes of receptors, the central-type benzodiazepine receptor (CBR) and the peripheral-type benzodiazepine receptor (PBR). CBR has been identified as a part of GABA_A receptor/Cl⁻ ionophore supramolecular complex, a pentameric protein, formed by different combinations of 21 distinct subunits (α_{1-6} , β_{1-4} , γ_{1-4} , θ , π , ϵ , ρ_{1-3} , δ), 16 of which have been found in the mammalian CNS. Allosteric modulation of GABA_A by CBR ligands involves three distinct events: ligand

binding to recognition site, transduction of the signal to the GABA effector site, modification in GABA-gated conductance². The peripheral-type benzodiazepine receptor (PBR), which was initially described as a binding site for the benzodiazepine diazepam present in peripheral tissues, is a 169-amino acid protein with five transmembrane domains of α -helices composed of 21 hydrophobic residues associated with the outer mitochondrial membrane. It is also located on the outer mitochondrial membrane in several organs including the kidney, nasal epithelium, lung, heart, and endocrine organs such as the adrenal, testis, and pituitary gland³⁻⁶. It is described as a multimeric complex composed of the 18 kDa molecular weight of isoquinoline binding receptor protein, the 34 kDa voltage-dependent anion channel (VDAC) protein required for benzodiazepine binding and the 30 kDa adenine nucleotide carrier of a yet unknown function in the complex⁷. Two additional proteins (10 kDa and PRAX-1) are believed to be involved in modulating PBR

functions⁸. The PBR complex being located at the contact site between the outer and the inner mitochondrial membranes, its subunit composition is thought to coincide with that of the mitochondrial permeability transition pore (PTP), which opens under specific conditions and enables unselective passage of molecules between the mitochondrial matrix and the cytoplasm⁹. The peripheral-type benzodiazepine-binding site (PBR), also known as the ω_3 binding site, is anatomically and pharmacologically distinct from the CBRs. They are highly expressed in steroidogenic tissues such as adrenal gland but also in kidney, heart, testis, and at a lower level in the brain parenchyma, ependyma, choroid plexus, and olfactory neurons¹⁰. Although the exact function of the PBR is not yet fully established, PBRs are involved in several functions such as cell proliferation, immune response modulation, regulation of mitochondrial oxidative phosphorylation, regulation of steroidogenesis and apoptosis¹¹. The peripheral benzodiazepine receptor (PBR) was overexpressed in a variety of tumors (e.g., certain brain tumors, ovarian cancer, liver tumors, breast carcinoma, colorectal cancer, etc.); this has led to the evaluation of PBR ligands as receptor mediated anticancer drug carriers to selectivity target to tumors. The receptor in neoplastic cells opens up the possibility of new pharmacological and diagnostic approaches in oncology^{12,13}. Increased concentrations of PBR were observed in lesion brain areas in a variety of neuropathological disorder such as multiple sclerosis, Alzheimer's disease, and Huntington's disease¹⁴⁻¹⁶. A wide variety of endogenous molecules have high affinities for PBR: they include the diazepam binding inhibitor (DBI) and its derived fragments, porphyrins (protoporphyrin IX, mesoporphyrin IX, hemin) and cholesterol. Specific synthetic PBR ligands can be divided into three families: i) benzodiazepines such as the 4'-chlorodiazepam (Ro5-4864), ii) isoquinoline carboxamides (PK14105, a photoaffinity ligand, and PK11195, which is one of the most powerful PBR ligands known) and iii) indolacetamide derivatives (for example, FGIN-1-27). Recently, an additional new specific PBR ligand, SSR180575, which is a pyridazinoindole derivative, has been reported. These ligands, which bind PBR with nanomolar affinities, were routinely used as pharmacological tools to characterize PBR properties and functions¹⁷. Ligands of benzodiazepine receptors (BzR) elicit a wide range of pharmacological effects. According to the efficacy,

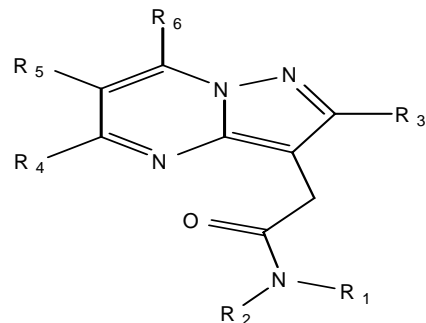
the ligands have been classified into agonist, inverse agonist, and antagonist corresponding to different pharmacological activity. Agonists (GABA-positive ligands), increasing the frequency of Cl^- channel opening, induce sedative/hypnotic, muscle relaxant, anticonvulsant and anxiolytic activities. Inverse agonists (GABA-negative ligands) decrease channel open frequency and display (pro)convulsant and anxiogenic activities. Antagonists do not exhibit, *per se*, any relevant biological effect but antagonize the action of agonists and inverse agonists. Based on thermodynamic features, Ro5-4864 was classified as an agonist whereas PK11195 was classified as an antagonist¹⁸⁻²¹. Useful information about PBR can be obtained from QSAR studies and the results of modeling of the putative endogenous PBR ligands and a subsequent comparison of their steric, electronic and lipophilic properties with those shared by high affinity synthetic ligands of PBR²².

Quantitative structure-activity relationship (QSAR) studies have been done on various derivatives acting on central and peripheral BzRs. Pharmacophore models have been reported for the acetamides²³ and flavonoids²⁴. Recently, Selleri *et al.*⁸ have reported a series of novel 2-phenylpyrazolo[1,5-a]pyrimidin-3-yl acetamides derivative as potent and selective ligands for PBR. In the present communication, the binding affinity data of the compounds for PBR have been subjected to QSAR studies with physiochemical and topological parameters to explore the requirements for PBR binding.

Materials and Methods

Peripheral and central benzodiazepine receptor (PBR) binding affinity data reported by Selleri *et al.*⁸ have been used as the model dataset for the present QSAR study: the affinity data $K_i(\text{nM})$ of 2-phenylpyrazolo[1,5-a]pyrimidin-3-yl acetamides series were converted to the logarithmic scale $[pK_i(\text{mM})]$ and then used for subsequent QSAR analyses as the response variable. There are six regions (**Table I**) of structural variations in the compounds: R_1 , R_2 and R_3 positions (showing diverse substitution pattern) and the R_4 , R_5 and R_6 positions (showing limited substitution pattern). The activity data (**Table I**) were subjected to QSAR analysis using linear free energy related (LFER) model of Hansch^{25,26} using lipophilicity (π), electronic parameter (Hammett σ), steric parameter (molar refractivity MR) and sterimol (L , B_1 , B_5) parameters

Table I—Structural features, physicochemical properties and PBR binding affinity values
2-phenylimidazo[1,2-a]pyrimidin-3-yl-acetamides



Sl. No.	R ₁	R ₂	R ₃	R ₄	R ₅	R ₆	logP _{calc}	MR	Obs ^a	cal ^b	cal ^c
1	Et	Et	Ph	Me	H	H	3.31	96.12	4.398	3.909	3.511
2	Et	Et	Ph	H	H	Me	2.94	96.13	3.810	3.550	3.652
3	Et	Et	Ph	Me	H	Me	3.64	101.07	4.538	4.533	4.524
4	Et	Et	4Cl-Ph	Me	H	Me	4.20	105.67	5.620	6.027	5.785
5	Et	Et	4F-Ph	Me	H	Me	3.80	101.47	5.036	5.119	5.457
6	Et	Et	4Me-Ph	Me	H	Me	4.13	106.96	6.097	5.952	5.746
7	Et	Et	4MeO-Ph	Me	H	Me	3.52	108.31	5.328	5.210	5.151
8	Et	Et	4F-Ph	Me	H	H	3.47	96.52	4.602	4.527	4.468
9	Et	Et	4Cl-Ph	H	H	Me	3.50	100.73	5.092	5.215	5.095
10	Et	Et	4Me-Ph	Me	H	CF ₃	4.77	107.57	6.046	5.725	5.660
11	Et	Et	4Me-Ph	CF ₃	H	Me	4.77	107.57	6.000	5.737	6.192
12	Et	Et	4MeO-Ph	CF ₃	H	CF ₃	4.80	109.53	4.796	5.099	5.735
13	Et	Et	4Cl-Ph	Me	H	Ph	5.60	125.37	5.620	6.007	5.446
14	Et	Et	4Cl-Ph	----	H	Me	3.50	100.73	5.469	5.215	5.095
15	Et	Et	4Cl-Ph	Me	Me	Me	4.69	111.57	5.215	5.073	5.158
16	Et	Et	4Cl-Ph	Me	COOEt	Me	4.36	122.72	5.076	4.807	4.982
17	Et	Et	4Me-Ph	H	Ph	H	4.77	122.67	4.244	4.019	4.057
18	Et	Et	Ph	Ph	H	H	4.70	115.81	3.648	4.428	4.263
19	Me	Me	4Me-Ph	Me	H	H	3.12	92.41	2.924	3.361	3.139
20	Me	Me	Ph	Me	H	Me	2.97	91.47	3.149	2.462	2.834
21	<i>n</i> -Pr	<i>n</i> -Pr	Ph	Me	H	Me	4.62	110.26	6.097	5.118	5.151
22	<i>i</i> -Pr	<i>i</i> -Pr	Ph	Me	Me	Me	4.77	116.34	4.051	4.687	4.389
23	<i>n</i> -But	<i>n</i> -But	Ph	Me	H	Me	5.45	119.46	5.347	5.280	5.322
24	<i>n</i> -Pentyl	<i>n</i> -Pentyl	Ph	Me	H	Me	6.29	128.66	5.097	5.134	5.177
25	<i>n</i> -hexyl	<i>n</i> -hexyl	Ph	Me	H	Me	7.12	137.86	4.638	4.688	4.719
26	<i>n</i> -octyl	<i>n</i> -octyl	Ph	Me	H	Me	8.79	156.26	2.949	2.886	2.850
27	Bz	Bz	Ph	Me	H	Me	6.19	139.62	4.398	4.380	4.684
28	Et	<i>i</i> -Pr	Ph	Me	H	Me	3.96	105.76	4.553	5.114	4.796
29	Et	Ph	Ph	Me	H	Me	4.97	115.35	6.097	4.831	4.887
30	Et	Bz	Ph	Me	H	Me	4.92	120.35	5.137	4.773	4.789
31	Me	(R)-CH ₂ CH ₃ Ph	Ph	Me	H	Me	5.02	120.65	4.658	4.479	4.268
32	Me	(S)-CH ₂ CH ₃ Ph	Ph	Me	H	Me	5.79	125.57	3.807	4.486	4.396
33	-(CH ₂) ₄ -	Ph	Me	H	Me	3.28	98.79	2.938	3.640	3.551	
34	-(CH ₂) ₅ -	Ph	Me	H	Me	3.70	103.39	3.517	4.020	3.902	
35	<i>n</i> -Pr	H	Ph	Me	H	Me	3.56	95.86	3.425	4.133	4.381

^a Taken from Ref. 8; ^b From Eq. (2); ^c From Eq. (6)

of the aryl ring substituents along with topological parameters and dummy parameters as predictor variables. The values of the physicochemical parameters, as listed in **Table II**, have been taken from reference²⁷. Some of the compounds reported in

the original paper were excluded in the present study because of the uncommon structural features. Hydrophobic whole molecular descriptor (partition coefficient $\log P_{calc}$) and molar refractivity (MR) were also tried as predictor variables. The software Chem

Draw Ultra ver 5.0 (ref. 28) was used for the calculation of $\log P_{calc}$ and MR values (Ghose and Crippen's fragmentation method²⁹). The calculated $\log P_{calc}$ and MR values for all compounds are given in **Table I**. The indicator and integer variables used in this study are defined in **Table III**.

The values for the topological and structural descriptors for the compounds has been generated by QSAR+ and Descriptor+ modules of the Cerius 2 version 4.8 software³⁰ from Accelrys (San Diego, USA) on a Silicon Graphics O2 workstation running under the IRIX 6.5 operating system. Various topological indices calculated are Balaban J , connectivity indices ($^0\chi$, $^1\chi$, $^2\chi$, $^3\chi_p$, $^3\chi_c$, $^0\chi^v$, $^1\chi^v$, $^2\chi^v$, $^3\chi_p^v$, $^3\chi_c^v$), kappa shape indices ($^1\kappa$, $^2\kappa$, $^3\kappa$, $^1\kappa_a$, $^2\kappa_a$, $^3\kappa_a$), E-state indices (S_sCH₃, S_ssCH₂, S_dsCH, S_aaCH, S_dssC, S_aasC, S_dCH₂, S_dO, S_ssO, S_sOH, S_sCl, S_sssN, S_ssNH, etc.) and structural parameters [Rotlbonds (number of rotatable bonds), hydrogen bond acceptors and hydrogen bond donors)].

The chemometric tools

For the development of equations, two methods were used: (1) stepwise regression, (2) multiple linear regressions with factor analysis as the data preprocessing step for variable selection (FA-MLR).

Table II — Different physiochemical parameters of aromatic substituents^a

Substituents		Substituent Constants				
R	π	MR	σ_p	B ₁	B ₅	L
H	0	0.103	0	1	1	2.06
Cl	0.71	0.60	0.23	1.8	1.8	3.52
CH ₃	0.56	0.56	-0.17	1.52	2.04	2.87
F	0.14	0.09	0.06	1.35	1.35	2.65
OCH ₃	-0.02	0.79	-0.27	1.35	3.07	3.98

^aTaken from ref. 27

Stepwise regression

In stepwise regression³¹, a multiple-term linear equation was built step-by-step. The basic procedures involve (1) identifying an initial model, (2) iteratively "stepping," that is, repeatedly altering the model at the previous step by adding or removing a predictor variable in accordance with the "stepping criteria," (in our case based on F for the forward selection method) and (3) terminating the search when stepping is no longer possible given the stepping criteria, or when a specified maximum number of steps has been reached. Specifically, at each step all variables are reviewed and evaluated to determine which one will contribute most to the equation. That variable will then be included in the model, and the process starts again. A limitation of the stepwise regression search approach is that it presumes there is a single "best" subset of X variables and seeks to identify it. There is often no unique "best" subset, and all possible regression models with a similar number of X variables as in the stepwise regression solution should be fitted subsequently to study whether some other subsets of X variables might be better.

FA-MLR

In case of FA-MLR, though multiple regression technique was used as the final statistical tool for developing QSAR relations, factor analysis^{32,33} was used as the data preprocessing step to identify the important predictor variables contributing to the response variable and to avoid collinearities among them. In a typical factor analysis procedure, the data matrix is first standardized, and correlation matrix and subsequently reduced correlation matrix are constructed. An eigen value problem is then solved and the factor pattern can be obtained from the corresponding eigen vectors. The principal objectives of factor analysis are to display multidimensional data in a space of lower dimensionality with minimum loss

Table III — Definitions of indicator and integer parameters

Parameter	Definition
I_{CF3_R4R6}	Indicator variable having value 1 if trifluoromethyl group is present at the R ₄ and R ₆ positions, value 0 otherwise
I_{CH3_R6}	Indicator variable having value 1 if methyl group is present at the R ₆ position, value 0 otherwise
I_{CH3_R4}	Indicator variable having value 1 if methyl group is present at the R ₄ position, value 0 otherwise
I_{CH3_R3}	Indicator variable having value 1 if methyl group is present at the R ₃ position, value 0 otherwise
I_{Ar_R3}	Indicator variable having value 1 if substituted phenyl group is present at the R ₃ position, value 0 otherwise
I_{Cl_R3}	Indicator variable having value 1 if chlorine atom is present at the R ₃ position, value 0 otherwise
I_{H_R6}	Indicator variable having value 1 if hydrogen atom is present at the R ₆ position, value 0 otherwise
N_{CH3_R1R2}	Number of methyl groups at R ₁ and R ₂ positions
N_{dieth_R1R2}	Number of ethyl groups at R ₁ and R ₂ positions
I_{R5}	Indicator variable having value 1 if any substitution group is present at R ₅ , value 0 otherwise

of information (explaining >95% of the variance of the data matrix) and to extract the basic features behind the data with ultimate goal of interpretation and/or prediction. The factors were extracted by principal component method and then rotated by VARIMAX rotation (a kind of rotation which is used in principal component analysis so that the axes are rotated to a position in which the sum of the variances of the loadings is the maximum possible) to obtain Thurston's simple structure. The simple structure is characterized by the property that as many variables as possible fall on the coordinate axes when presented in common factor space, so that largest possible number of factor loadings becomes zero. This is done to obtain a numerically comprehensive picture of the relatedness of the variables. Only variables with non-zero loadings in such factors where biological activity also has non-zero loading were considered important in explaining variance of the activity. Furthermore, variables with non-zero loadings in different factors were combined in a multivariate equation.

The factor analysis (FA) and multiple regression analysis (MLR) were performed using the statistical software SPSS³⁴. The statistical quality of the equations³⁵ was judged by the parameters like *explained variance* (R_a^2 , i.e., *adjusted R*²), *correlation coefficient* (r or R), *standard error of estimate* (s), *variance ratio* (F) at specified degrees of freedom (df) and 95% confidence intervals of the regression coefficients. All accepted equations have regression coefficients and F ratios significant at 95% and 99% levels respectively, if not stated otherwise (marked with*). A compound was considered as an outlier if the residual is more than twice the standard error of estimate for a particular equation. The generated QSAR equations were validated by PRESS (leave-one-out)^{36,37} statistics using MINITAB software³⁸ and the reported parameters are *cross-validation R*² (Q^2), *predicted residual sum of squares* (PRESS), *standard deviation based on PRESS* (S_{PRESS})³⁹ and *standard deviation of error of prediction* ($SDEP$)³⁹. Finally, 'leave-25%-out' was also applied on some selected equations to show robustness and predictive potential of the generated equations.

Results and Discussion

Stepwise Regression

Using stepping criteria based on F value, the following two equations were derived with seven and six variables respectively:

$$\begin{aligned}
 pK_i = & 2.735(\pm 0.929) \log P_{calc} - 0.235(\pm 0.082)[\log P_{calc}]^2 \\
 & + 1.010(\pm 0.698) BI_{p_R3} + 0.136(\pm 0.137) S_aasC \\
 & + 2.436(\pm 1.559) JX - 0.633(\pm 0.392) N_{CH3_R1R2} \\
 & - 1.330(\pm 0.694) I_{R5} - 8.993(\pm 4.610) \\
 n = & 35, R_a^2 = 0.692, R^2 = 0.755, R = 0.869, \\
 F = & 12.9(df 7, 27), s = 0.537, Q^2 = 0.595, \\
 SDEP = & 0.607, S_{PRESS} = 0.691, PRESS = 12.9 \\
 & \dots \quad (1)
 \end{aligned}$$

The 95% confidence intervals of the regression coefficients are mentioned within parentheses. Eq. (1) can explain and predict 69.2% and 59.5% respectively of the variance of the PBR binding affinity. The partition coefficient shows a parabolic relation with the PBR binding affinity. This suggests that the binding affinity increases with increase in the partition coefficient of the compounds until it reaches the critical value after which the affinity decreases. The critical value of $\log P_{calc}$ is 5.819. The positive coefficient of BI_{p_R3} indicates that the width of the *para* substituents is conducive for the binding affinity. The positive coefficient of S_aasC shows that the binding affinity increases with increase in the E-state

values of the fragment . The positive coefficient of the average distance sum connectivity (Balaban J) signifies the importance of relative distance among different groups. The negative coefficient of N_{CH3_R1R2} shows that the presence of methyl groups at R_1 and R_2 are detrimental to the binding affinity. The negative coefficient of I_{R5} shows that the presence of substituents at R_5 position is detrimental to the binding affinity. The intercorrelation (r) matrix among the predictor variables used in Eq. (1) is given in **Table IV**.

$$\begin{aligned}
 pK_i = & 2.332(\pm 0.850) \log P_{calc} - 0.215(\pm 0.078)[\log P_{calc}]^2 \\
 & + 1.426(\pm 0.615) BI_{p_R3} + 0.170(\pm 0.096) S_sCH_3 \\
 & - 0.688(\pm 0.371) N_{CH3_R1R2} - 1.522(\pm 0.680) I_{R5} \\
 & - 3.892(\pm 2.410) \\
 n = & 35, R_a^2 = 0.718, R^2 = 0.768, R = 0.876, \\
 F = & 15.4(df 6, 28), s = 0.513, Q^2 = 0.613, \\
 SDEP = & 0.593, S_{PRESS} = 0.663, PRESS = 12.3 \\
 & \dots \quad (2)
 \end{aligned}$$

Eq. (2) can explain and predict 71.8% and 61.3% respectively of the variance of the PBR binding

Table IV—Intercorrelation (*r*) matrix for topological, physiochemical and indicator variables of Eqs (1) and (2)

	<i>logP_{calc}</i>	<i>[logP_{calc}]²</i>	<i>JX</i>	<i>N_{CH3_RIR2}</i>	<i>I_{R5}</i>	<i>S_aasC</i>	<i>BI_{P_R3}</i>	<i>S_sCH₃</i>
<i>logP_{calc}</i>		0.984	-0.528	-0.195	0.031	0.092	-0.194	0.149
<i>[logP_{calc}]²</i>	0.984		-0.513	-0.156	-0.014	0.093	-0.219	0.138
<i>JX</i>	-0.528	-0.513		0.041	0.161	-0.355	0.450	0.412
<i>N_{CH3_RIR2}</i>	-0.195	-0.156	0.041		-0.122	0.128	-0.084	0.058
<i>I_{R5}</i>	0.031	-0.014	0.161	-0.122		0.270	0.318	0.448
<i>S_aasC</i>	0.092	0.093	-0.355	0.128	0.270		-0.059	0.351
<i>BI_{P_R3}</i>	-0.194	-0.219	0.450	-0.084	0.318	-0.059		0.073
<i>S_sCH₃</i>	0.149	0.138	0.412	0.058	0.448	0.351	0.073	

affinity. The critical value of *logP_{calc}* is 5.423. The positive coefficient of *S_sCH₃* shows that the binding affinity increases with increase in the E-state values of the methyl fragment. The calculated binding affinity values according to Eq. (2) are given in **Table I**. Leave-25%-out crossvalidation was also applied on Eq. (2); the average regression coefficients for the different variables and the corresponding standard deviations for the four cycles are shown in **Table V**. The intercorrelation (*r*) matrix among the predictor variables used in Eq. (2) is given in **Table IV**.

FA-MLR

The peripheral benzodiazepine receptor binding affinity, topological parameters, physiochemical substituent constants of the phenyl ring and the indicator/integer descriptors along with hydrophobic and steric whole molecular descriptors partition coefficient (*logP_{calc}*), and molar refractivity (*MR*) were subjected to the factor analysis. The results of the factor analysis showed that eleven factors could explain 95.8% of the variance of the binding affinity. Different factors (arranged in order of decreasing importance) in which the binding affinity shows non-zero loadings are: factor 11 (loaded in *N_{CH3_RIR2}*), Factor 3 (loaded in *BI_{P_R3}*), factor 8 (loaded in *I_{CH3_R6}*, *I_{H_R6}*), factor 9 (loaded in *I_{Ar_R3}*, *σ_{P_R3}*), factor 4 (loaded in *H_bond_donor*, *chiral_centers*, *S_ssNH* and *S_sssN*), factor 2 (loaded in *S_sCl*, χ_c , *SC_3_C*, *S_aasC*, *S_aaaC*), factor 10 (loaded in *S_ssO*). The binding affinity is poorly loaded with other factors (1, 5, 6, 7). Based on the results of the factor analysis (Table not shown), the following equation with seven variables was derived:

$$\begin{aligned}
 pK_i = & 3.053(\pm 0.985) \log P_{calc} - 0.259(\pm 0.086)[\log P_{calc}]^2 \\
 & + 0.145(\pm 0.177)S_{ssssC} + 2.552(\pm 1.580)JX \\
 & - 1.224(\pm 0.663)I_{R5} - 0.582(\pm 0.386)N_{CH3_RIR2} \\
 & + 0.700(\pm 0.458)I_{Ar_R3} - 8.502(\pm 4.779) \\
 n = & 35, R_a^2 = 0.693, R^2 = 0.756, R = 0.870, \\
 F = & 12.0(df 7, 27), s = 0.536, Q^2 = 0.562, \\
 SDEP = & 0.630, S_{PRESS} = 0.718, PRESS = 13.9 \\
 & \dots \quad (3)
 \end{aligned}$$

The 95% confidence intervals of the regression coefficients are mentioned within parentheses. Eq. (3) can explain and predict 69.3% and 56.2% respectively of the variance of the PBR binding affinity. The partition coefficient shows parabolic relation with the activity. This suggests that the binding affinity increases with increase in the value of partition coefficient of the compounds until it reaches the critical value after which the affinity decreases. The critical value of *logP_{calc}* is 5.894. The positive coefficient of *S_sssssC* shows that the binding affinity increases with increase in the E-state values of the

fragment . The positive coefficient of *I_{Ar_R3}* shows that the presence of substituents at R₃ is conducive to the binding affinity.

When the term *S_sssssC* is replaced with *S_sF* in Eq. (3), marginal increase in the quality was observed.

$$\begin{aligned}
 pK_i = & 3.050(\pm 0.971) \log P_{calc} - 0.259(\pm 0.086)[\log P_{calc}]^2 \\
 & - 0.019(\pm 0.014)S_{sF} + 2.582(\pm 1.563)JX \\
 & - 1.272(\pm 0.666)I_{R5} - 0.598(\pm 0.382)N_{CH3_RIR2} \\
 & + 0.751(\pm 0.462)I_{Ar_R3} - 8.545(\pm 4.702) \\
 n = & 35, R_a^2 = 0.699, R^2 = 0.761, R = 0.872, \\
 F = & 12.3(df 7, 27), s = 0.530, Q^2 = 0.571, \\
 SDEP = & 0.623, S_{PRESS} = 0.710, PRESS = 13.6 \\
 & \dots \quad (4)
 \end{aligned}$$

Table V—Intercorrelation (r) matrix for topological, physiochemical and indicator variables of Eqs (3), (4), (5) and (6)

	$\log P_{calc}$	$[\log P_{calc}]^2$	JX	N_{CH3_R1R2}	I_{CH3_R6}	I_{Ar_R3}	I_{R5}	S_sssN	S_ssssC
$\log P_{calc}$		0.98	-0.53	-0.20	0.10	-0.24	0.03	0.15	-0.06
$[\log P_{calc}]^2$	0.98		-0.51	-0.16	0.11	-0.26	-0.01	0.16	-0.02
JX	-0.53	-0.51		0.04	-0.11	0.51	0.16	0.01	-0.34
N_{CH3_R1R2}	-0.20	-0.16	0.04		-0.08	-0.07	-0.12	-0.06	0.10
I_{CH3_R6}	0.10	0.11	-0.11	-0.08		-0.35	-0.02	0.01	0.36
I_{Ar_R3}	-0.24	-0.26	0.51	-0.07	-0.35		0.23	0.04	-0.32
I_{R5}	0.03	-0.01	0.16	-0.12	-0.02	0.23		0.11	0.10
S_sssN	0.15	0.16	0.01	-0.06	0.01	0.04	0.11		0.16
S_ssssC	-0.06	-0.02	-0.34	0.10	0.36	-0.32	0.10	0.16	

Table VI—Results of leave-25%-out cross-validation applied on Eqs.(2) and (6) Model equation, $pC = \Sigma \beta_i x_i + \alpha$.

Eq. No	No. of cycles	Average regression coefficients (\pm standard deviations)	Q^2 Statistic (Average Pres)
2	4 ^a	$2.074(\pm 1.105)\log P_{calc} - 0.169(\pm 0.149)[\log P_{calc}]^2 - 0.470(\pm 0.512)I_{Ar_R3}$ $+1.148(\pm 0.623)S_sCH_3 - 1.043(\pm 1.019)N_{CH3_R1R2}$ $+0.150(\pm 0.062)I_{R5} - 3.052(\pm 3.067)$	0.583 (0.487)
6	4 ^a	$2.838(\pm 0.433)\log P_{calc} - 0.249(\pm 0.042)[\log P_{calc}]^2 + 1.642(\pm 0.304)JX$ $-0.523(\pm 0.062)N_{CH3_R1R2} + 0.581(\pm 0.242)I_{CH3_R6} + 0.770(\pm 0.279)I_{Ar_R3}$ $-1.009(\pm 0.195)I_{R5} - 6.540(\pm 1.087)$	0.540 (0.507)

Q^2 denotes cross-validated R^2 . Average Pres means average of absolute values of *predicted residuals*.

^a Compounds were deleted in 4 cycles in the following manner: (1, 5, 9,...,33), (2, 6, 10,...,34), (3, 7, 11,...,35), (4, 8, 12,...,32),

Eq. (4) can explain and predict 66.8% and 57.5% respectively of the variance of the PBR activity data. The negative coefficient of S_sF shows that the E-state value of the fragment -F is detrimental to the binding affinity. The critical value of $\log P_{calc}$ according to Eq. (4) is 5.880. There was further improvement in the quality of the model when S_sssN was introduced in place of S_sF .

$$\begin{aligned}
 pK_i = & 2.516(\pm 0.934)\log P_{calc} - 0.229(\pm 0.086)[\log P_{calc}]^2 \\
 & + 0.447(\pm 0.551)S_sssN - 0.964(\pm 0.648)I_{R5} \\
 & + 0.617(\pm 0.496)I_{CH3_R6} - 0.519(\pm 0.402)N_{CH3_R1R2} \\
 & + 0.998(\pm 0.447)I_{Ar_R3} - 3.176(\pm 2.706) \\
 n = & 35, R_a^2 = 0.668, R^2 = 0.737, R = 0.858, \\
 F = & 10.8(df 7, 27), s = 0.557, Q^2 = 0.575, \\
 SDEP = & 0.621, S_{PRESS} = 0.707, PRESS = 13.5
 \end{aligned} \quad \dots \quad (5)$$

Eq. (5) can explain and predict 66.8% and 57.5% respectively of the variance of the PBR binding

affinity. The critical value of $\log P_{calc}$ according to Eq. (5) is 5.493. Further improvement in the predicted variance of the model was obtained when S_sssN was introduced in place of S_sF , but explained variance decreased.

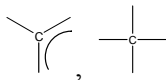
$$\begin{aligned}
 pK_i = & 2.672(\pm 0.929)\log P_{calc} - 0.232(\pm 0.084)[\log P_{calc}]^2 \\
 & + 1.580(\pm 1.460)JX - 0.521(\pm 0.392)N_{CH3_R1R2} \\
 & + 0.573(\pm 0.486)I_{CH3_R6} + 0.791(\pm 0.484)I_{Ar_R3} \\
 & - 0.993(\pm 0.634)I_{R5} - 6.041(\pm 4.262) \\
 n = & 35, R_a^2 = 0.686, R^2 = 0.751, R = 0.867, \\
 F = & 11.6(df 7, 27), s = 0.541, Q^2 = 0.594, \\
 SDEP = & 0.607, S_{PRESS} = 0.691, PRESS = 12.9
 \end{aligned} \quad \dots \quad (6)$$

Eq. (6) can explain and predict 68.6% and 59.4% respectively of the variance of the PBR binding affinity. By replacing S_sssN with I_{Ar_R3} in Eq. (5) considerable rise in the quality of the model resulted. The positive coefficient of I_{CH3_R6} shows that the presence of methyl group at R₆ is conducive to the binding affinity. The critical value of $\log P_{calc}$

according to Eq. (6) is 5.759. The calculated binding affinity values according to Eq. (6) are given in **Table I**. The intercorrelation (r) matrix among the predictor variables used in Eq. (3), (4), (5) and (6) is given in **Table V**. Eq. (6) involves seven descriptors for 35 data points and thus maintains the recommended ratio of number of descriptors to number of data point of 1:5. Furthermore, the leave-one-out Q^2 value is more than the recommended cut-off value of 0.5^{40,41}. Leave-25%-out crossvalidation was also applied on Eq. (6); the average regression coefficients for the different variables and the corresponding standard deviations for the four cycles are shown in **Table VI**. Crossvalidation statistics indicate robustness of the formulated models.

Conclusions

The present QSAR study has explored the structural and physicochemical requirements of 2-phenylimidazo[1,2- a]pyrimidin-3-yl-acetamides as peripheral benzodiazepine receptor ligands. The $\log P_{\text{calc}}$ parameter shows a parabolic relation with the peripheral benzodiazepine receptor binding affinity, which suggests that the binding affinity increases with increase in the partition coefficient of the compounds until it reaches the critical value after which the affinity decreases. The range of the critical value of $\log P$ is within 5.423-5.819. The width of the *para* substituents at R_3 is conducive for the binding affinity. The E-state values of the fragments like



methyl, , and

are conducive for the binding affinity, while E-state values of the fragment of -F is detrimental to the binding affinity. The average distance sum of the connectivity (Balaban J) among different groups is also conducive for the binding affinity. The presence of methyl groups at R_1 and R_2 positions and presence of substituents at R_5 position are detrimental to the binding affinity, while presence of substituents at R_3 position and presence of methyl group at R_6 position are conducive to the binding affinity.

Acknowledgements

One of the authors (MKD) thanks the AICTE, New Delhi for a QIP fellowship. KR thanks the AICTE, New Delhi for a financial grant under the Career Award for Young Teachers scheme. Thanks are also due to Paola Gratteri (Universita` di Firenze, Firenze, Italy) for providing us with the reprint of their work.

References

- 1 Szewczyk A & Wojtczak L, *Pharmacol Rev*, 54, **2002**, 101.
- 2 Campagna F, Palluotto F, Carotti A & Maciocco E, *Il Farmaco*, 59, **2004**, 849.
- 3 Braestrup C & Squires R F, *Proc Natl Acad Sci*, 74, **1977**, 1839.
- 4 Joseph-Liauzun E, Delmas P, Shire D & Ferrara P, *J Biol Chem*, 273, **1998**, 2146.
- 5 Vin V, Leducq N, Bono F & Herbert J M, *Biochem Biophys Res Commun*, 310, **2003**, 785.
- 6 Zhang M R, Ogawa J M M, Noguchi J, Ito T, Yoshida Y, Okauchi T, Obayashi S, Suhara T & Suzuki K, *J Med Chem*, 47, **2004**, 2228.
- 7 Lacape`re J J, Delavoie F, Li H, Pe`ranzi G, Maccario J, Papadopoulos V & Vidic B, *Biochem Biophys Res Commun*, 284, **2001**, 536.
- 8 Selleri S, Gratteri P, Costagli C, Bonaccini C, Costanzo A, Melani F, Guerrini G, Ciciani G, Costa B, Spinetti F, Martini C & Bruni F, *Bioorg Med Chem*, 13, **2005**, 4821.
- 9 Marselli L, Trincavelli L, Santangelo C, Lupi R, Guerra S D, Boggi U, Falleni A, Gremigni V, Mosca F, Martini C, Dotta F, Mario U D, Prato S D & Marchetti P, *European Journal of Endocrinology*, 151, **2004**, 207.
- 10 Matarrese M, Moresco R M, Cappelli A, Anzini M, Vomero S, Simonelli P, Verza E, Magni F, Sudati F, Soloviev D, Todde S, Carpinelli A, Kienle M G & Fazio F, *J Med Chem*, 44, **2001**, 579.
- 11 Campagna F, Palluotto F, Mascia M P, Maciocco E, Marra C, Carotti A & Carrieri A, *Il Farmaco*, 58, **2003**, 129.
- 12 Roy K, De A U & Sengupta C, *Indian J Biochem Biophys*, 40, **2003**, 203.
- 13 Cappelli A, Mohr G P, Gallelli A, Giuliani G, Anzini M, Vomero S, Fresta M, Porcu P, Maciocco E, Concias A, Biggio G & Donat A, *J. Med. Chem.*, 46, **2003**, 3568.
- 14 Diorio D, Welner S A, Butterworth R F, Meaney M J & Suranyi-Cadotte B E, *Neurobiol Aging*, 12, **1991**, 255.
- 15 Be`navide`s J, Cornu P, Dennis T, Dubois A Hauw J J, MacKenzie E T, Sazdovitch V & Scatton B, *Ann Neurol*, 24, **1988**, 708.
- 16 Vowinckel E, Reutens D, Becher B, Verge G, Evans A, Owens T & Antel J P, *J Neurosci Res*, 50, **1997**, 345.
- 17 Galiegue S, Tinel N & Casellas P, *Curr Med Chem*, 16, **2003**, 1563.
- 18 Hadingham K L, Wingrove P, Le-Bourdelle B, Palmer K J, Ragan C I & Whiting P J, *Mol Pharmacol*, 43, **1993**, 970.
- 19 Whiting J G, McKernan R M & Iversen L L, *Proc Natl Acad Sci*, 87, **1990**, 9966.
- 20 Doble A & Martin I L, *Trends Pharmacol Sci*, 13, **1992**, 76.
- 21 Tulinsky J & Gammill L B, *Curr Med Chem*, 3, **1994**, 226.
- 22 Cinonea N, Höltjeb H D & Carottia A, *Journal of Computer-Aided Molecular Design*, 14, **2000**, 753.
- 23 (a) Trapani G, Laquintana V, Denora N, Trapani A, Lopedota A, Latrofa A, Franco M, Serra M, Pisu M G, Floris I, Sanna E, Biggio G & Liso G, *J Med Chem*, 48, **2005**, 292.
(b) Dalai M K, Leonard J T & Roy K, *Indian J Biochem Biophys*, 43, **2006**, 105

24 Huang X, Liu T, Gu J, Luo X, Ji R, Cao Y, Xue H, Wong J T, Wong B L, Pei G & Jiang H, *J Med Chem* 44, **2001**, 1883.

25 Hansch C & Fujita T, *J Am Chem Soc*, 86, **1964**, 1616.

26 Kubinyi H, *Methods and Principles in Medicinal Chemistry* edited by H Timmerman, R Mannhold & P Krogsgaard-Larsen, (VCH, Weinheim) **1993**.

27 Kubinyi H, *Burger's Medicinal Chemistry and Drug Discovery*, edited by M. E. Wolff, (John Wiley & Sons, New York) **1995**, pp 507–509.

28 *Chem Draw Ultra version5.0 and Chem 3D Pro version5*. (Cambridge soft Corporation, USA).

29 Ghose A K & Crippen G M, *J Chem Inf Compu. Sci*, 27, **1987**, 21.

30 Cerius² ver. 4.8 (Accelrys, Inc., San Diego, USA).

31 Darlington RB, *Regression and linear models* (McGraw-Hill, New York) **1990**.

32 Franke R, *Theoretical Drug Design Methods*, (Elsevier, Amsterdam) **1984**, pp184-195.

33 Franke R & Gruska A in *Chemometric Methods in Molecular Design* edited by H van de Waterbeemd, (VCH, Weinheim) **1995**, pp 113-163.

34 SPSS is statistical software of SPSS Inc., IL, USA.

35 Snedecor G W & Cochran W G, *Statistical Methods*, (Oxford & IBH Publishing Co. Pvt. Ltd, New Delhi) **1967**, pp 381-418.

36 Wold S & Eriksson L in *Chemometric Methods in Molecular Design* edited by H van de Waterbeemd, (VCH, Weinheim) **1995**, pp 312-317.

37 Debnath A K & Ghose A K in *Combinatorial Library design and Evaluation* edited by A K Ghosh & V N Viswanadhan, (Marcel Dekker, Inc. New York) **2001**, pp 73-129.

38 MINITAB is a statistical software of Minitab Inc, USA.

39 Debnath A K in *Combinatorial Library design and Evaluation* edited by A K Ghosh & V N Viswanadhan, (Marcel Dekker, Inc. New York) **2001**, pp 73-129.

40 Walker J D, Jaworska J, Comber M H, Schultz T W & Dearden J C, *Environ Toxicol Chem* 22, **2003**, 1653.

41 Eriksson L, Jaworska J, Worth A P, Cronin M T D, McDowell R M & Gramatica P, *Environ Health Perspect*, 111, **2003**, 1361.